A Simple Model for the Pacific Cold Tongue and ENSO*

F.-F. JIN

Department of Meteorology, School of Ocean and Earth Science and Technology, University of Hawaii at Manoa, Honolulu, Hawaii

(Manuscript received 2 December 1996, in final form 15 October 1997)

ABSTRACT

A conceptual model is constructed based upon the Bjerknes hypothesis of tropical atmosphere–ocean interaction. It is shown that strong feedbacks among the trade winds, equatorial zonal sea surface temperature contrast, and upper-ocean heat content occur in the tropical Pacific basin. Coupled atmosphere–ocean dynamics produce both the strong Pacific cold-tongue climate state and the El Niño–Southern Oscillation (ENSO) phenomenon. The cold-tongue climate state is unstable and gives rise to the self-sustained ENSO, which can be understood as an equatorial ocean recharge oscillator. The small basin size and the influence of a wind system resulting from heating sources of its adjacent landmasses are responsible for a weak and stable Atlantic cold-tongue state that cannot support ENSO-like interannual variability. The presence of westerly wind associated with the Walker circulation ascending at the western Pacific warm pool disables the dynamical coupling processes in the equatorial Indian Ocean. As a result, the equatorial Indian Ocean maintains a stable warm climate state. The conceptual coupled model reproduces the basic features of the climate states of the tropical Pacific, Atlantic, and Indian Ocean basins and the dominant interannual climate variability of the tropical climate system.

1. Introduction

The tropical Pacific features the large zonal contrast in SST along the equator, with a warm pool in the west and a cold tongue in the east, and the strong SST interannual fluctuations in the cold tongue region. This interannual variabilty is dominated by the well-known ENSO phenomenon, which affects much of the global climate (Rasmusson and Wallace 1983). Great progress has been made over the past decade in understanding and predicting ENSO (Philander et al. 1984; Cane and Zebiak 1985; Anderson and McCreary 1985; Cane et al. 1986; Zebiak and Cane 1987; Barnett et al. 1988; Battisti 1988; Battisti and Hirst 1989; Suarez and Schopf 1988; Schopf and Suarez 1988; Philander 1990; Barnett et al. 1991; Neelin 1991; Philander et al. 1992; Jin and Neelin 1993; Neelin et al. 1994; Latif et al. 1994; Neelin et al. 1998; Jin 1997a,b).

Bjerknes (1969) first hypothesized that a positive feedback of tropical ocean–atmosphere interaction can amplify SST perturbations of the cold tongue to sustain either a warm or a cold phase of ENSO. The easterly trade winds force the thermocline depth to be shallower in the equatorial eastern Pacific than in the western Pacific. The trade winds also induce the equatorial Ekman upwelling, which effectively brings cold water from the subsurface to the surface layer to generate a cold tongue in the eastern Pacific. The atmospheric zonal pressure gradient caused by the east–west contrast of the SST drives an equatorial zonally asymmetric circulation—the Walker circulation, which enhances the surface easterlies over the Pacific basin and thus strengthens the cold tongue. However, Bjerknes was unable to uncover the phase transition mechanism for ENSO. It was found nearly two decades later that during warm (cold) ENSO phases, the equatorial heat content is often draining out (building up) as a result of the mass exchange between the equatorial belt and off-equatorial regions through oceanic dynamical adjustment (Cane and Zebiak 1985; Wyrtki 1985; Cane et al. 1986). It was proposed (Cane and Zebiak 1985; Wyrtki 1985; Cane et al. 1986) that discharge/recharge of the equatorial heat content, which is out of phase with SST anomalies of ENSO, was responsible for ENSO phase transitions. Jin (1997a) showed that this recharge-oscillation mechanism is at the heart of ENSO theory pointing to the instability of the tropical Pacific climate state, which supports a delayed oscillator (Schopf and Suarez 1988; Battisti and Hirst 1989) or a mixed SST–ocean dynamics mode (Jin and Neelin 1993).

While ENSO research has been focusing on anomalies of the tropical coupled system, understanding the totality of the coupled dynamics of both the climate state

* School of Ocean and Earth Science and Technology Contribution Number 4630.

Corresponding author address: Dr. Fei-Fei Jin, Dept. of Meteorology, School of Ocean and Earth Science and Technology, University of Hawaii at Manoa, 2525 Correa Rd., Honolulu, HI 96822-2219.
E-mail: jff@kukui.soest.hawaii.edu

and the variability of the tropical climate system becomes a new challenge. Significant progress has been made in coupled climate modeling by avoiding artificial restoration of climate states of coupled general circulation models to the observed state (e.g., Mechoso et al. 1995) so that the models consistently simulate both the climate-mean state and its variability. Recent work further suggested that the Bjerknes positive feedback hypothesis not only sets the foundation for ENSO theory but also offers an explanation for the genesis of the Pacific cold tongue in the time-mean climate state of the tropical Pacific (Dijkstra and Neelin 1995; Sun and Liu 1996; Jin 1996). It was further illustrated by Jin (1996) that the ENSO phenomenon and the Pacific cold tongue, the two intimately related aspects of tropical climate, can be depicted in one unified paradigm. Therefore, decades of research have brought us to the point where both ENSO and the Pacific warm pool/cold tongue climate state can be understood in a unified manner as first envisioned by Bjerknes (1969).

In this paper, the simple conceptual coupled model of Jin (1996), which reproduces the basic features of both Pacific cold tongue and ENSO, is extended and the sensitivity of the Pacific cold tongue state and its stability to various physical processes are closely examined. This paper will be organized as follows. The model is developed in section 2. The sensitivity of both the climate state and the ENSO-like oscillation to various processes will then be explored in section 3. Discussions on the equatorial Atlantic and Indian Ocean climate states and the conclusions will be given in sections 4 and 5, respectively.

2. Model

To illustrate the essential mechanisms for both the Pacific warm pool/cold tongue climate state and the ENSO, a coupled two-box model is constructed based on the hypotheses of Bjerknes (1969), Wyrtki (1985), and Cane and Zebiak (1985) (hereafter, collectively referred as BWCZ) to depict the positive feedback of the tropical ocean–atmosphere interaction and the subsurface memory in the ocean dynamic adjustment. The equatorial Pacific basin was divided into an eastern and a western half to distinguish the cold tongue and the warm pool. The temperatures of the well-mixed surface layer of the western and eastern basins are then controlled by

$$\frac{dT_w}{dt} = -\varepsilon_T(T_w - T_r) + M(-u)(T_e - T_w)/(L/2), \quad (1a)$$

$$\frac{dT_e}{dt} = -\varepsilon_T(T_e - T_r) - M(w)(T_e - T_{se})/H_m,$$

$$M(x) = \begin{cases} 0, & x \le 0 \\ x, & x > 0. \end{cases} \quad (1b)$$

The first terms on the right-hand side of Eqs. (1a) and (1b) represent the net heating due to radiative, sensible, and latent heat fluxes through the ocean surface. This net heating is parameterized by a collective feedback parameter ε_T, which measures the rate at which the SST is restored to a zonally uniform radiative–convective equilibrium temperature ($T_r = 30°C$). The second term on the right side of Eq. (1a) represents SST zonal advection and the second term in Eq. (1b) represents dynamical cooling due to the upwelling of the cold subsurface water (at temperature T_{se}) into the surface layer. Zonal and upwelling velocities are denoted by u and w, while L and H_m are the basin width and the mixed-layer depth (about 50 m). The function $M(x)$ results from upstream differencing. The poleward surface currents, which compensate for a large part of the equatorial upwelling in the eastern box do not alter the equatorial SST.

The relatively small surface zonal current is assumed to be proportional to zonal wind stress τ and the zonal advective timescale is thus

$$u/(L/2) = a_d\alpha\tau, \quad (2)$$

where a_d, as shown in the appendix, is a small nondimensional parameter measuring the zonal advective feedback, and parameter α depends on the latitudinal variation of the Coriolis parameter and the momentum mixing rate in the upper ocean.

The equatorial upwelling is largely due to Ekman flow divergence, which includes both contributions from the surface poleward and westward flow. As shown in Neelin (1991) and Jin and Neelin (1993), the divergence due to poleward Ekman flow dominates the equatorial upwelling and this part of the upwelling is largely proportional to the zonal wind stress. Thus, the total upwelling rate, as also shown in the appendix, can be expressed as

$$w/H_m = -\alpha\tau(1 + a_d). \quad (3)$$

The equatorial zonal wind stress in Eq. (2) is divided into three parts:

$$\tau = \tau_W + \tau_H + \tau_{EX}, \quad (4)$$

representing the contributions from the Walker circulation, the Hadley circulation, and an external component of zonal flow, respectively. The Walker circulation ascends over the western Pacific warm pool and descends over the eastern Pacific cold-tongue region, driving an easterly surface wind over the equatorial Pacific. The approximate balance between the adiabatic warming as a result of the descending motion of the Walker circulation and the heat loss to the underlying cold surface implies that the intensity of the Walker circulation is closely related to zonal contrast of atmospheric heating. Thus, we can express

$$\tau_W = -a_W(T_w - T_e). \quad (5)$$

By considering horizontal eddy momentum transport, a symmetric Hadley cell may accompany a weak equa-

torial surface easterly. The zonal wind stress component due to the Hadley circulation, which is driven by meridional differential heating, thus can be expressed as

$$\tau_{\rm H} = -a_{\rm H}(T_w + T_e - 2T_n)/2, \quad (6)$$

where T_n is the subtropical SST and parameters $a_{\rm W}$, $a_{\rm H}$ are feedback coefficients that measure the efficiency of the zonal and meridional heating contrasts in driving the Walker and Hadley circulation. The external part of zonal wind stress represents the zonal wind induced by heating sources over adjacent landmasses or an ocean basin. For the convenience of discussion, in the following, we define $\mu = \alpha a_{\rm W}$ as a dynamical coupling coefficient, $\mu_{\rm H} = a_{\rm H}/a_{\rm W}$ as a nondimensional relative feedback coefficient for the Hadley circulation, and $\tau_{\rm EX} = -\mu\Delta T$ with a specified ΔT in the dimensional unit of degrees Celsius. Equation (4) can be rewritten as

$$\tau = -\mu/\alpha\{(T_w - T_e) + \mu_{\rm H}(T_w + T_e - 2T_n)/2 + \Delta T\}. \quad (7)$$

The subsurface temperature depends strongly on the thermocline depth. By considering a typical vertical temperature profile of the tropical Pacific, it can be parameterized as in Jin et al. (1996),

$$T_{se} = T_r - (T_r - T_{r0})[1 - \tanh(H + h_e - z_0)/h^*)]/2, \quad (8)$$

where $T_{r0} = 18$°C is the temperature beneath the thermocline, h_e is the departure of thermocline depth in the eastern equatorial Pacific from its reference depth $H = 100$ m, $z_0 = 75$ m is the depth at which w takes its characteristic value, and $h^* = 50$ m measures the sharpness of the thermocline.

The Sverdrup balance (Philander 1990) between the pressure gradient force and wind stress over the equator constrains the east–west contrast of the thermocline depth

$$h_e = h_w + bL\tau, \quad (9)$$

where h_w denotes the departure of the thermocline depth in the western equatorial Pacific from the reference depth H; $bL\tau$ is proportional to the zonally integrated wind stress in the equatorial region; L is the ocean basin size; and b measures the efficiency of wind stress in driving the thermocline tilt. Thermocline depth h_w adjusts slowly to the zonally integrated Sverdrup meridional mass transport resulting from the wind-forced equatorial Rossby waves, and follows the equation

$$\frac{dh_w}{dt} = -rh_w - rbL\tau/2. \quad (10)$$

Parameter r measures the basinwide dynamic adjustment rate, $rbL\tau/2$ represents the zonally integrated Sverdrup meridional mass transport, and the factor $r/2$ in this term constrains the zonal-mean thermocline depth at the equilibrium state to be the same as the reference depth. Conceptually, this equation simply describes the slow dynamic renewal of the warm pool heat content.

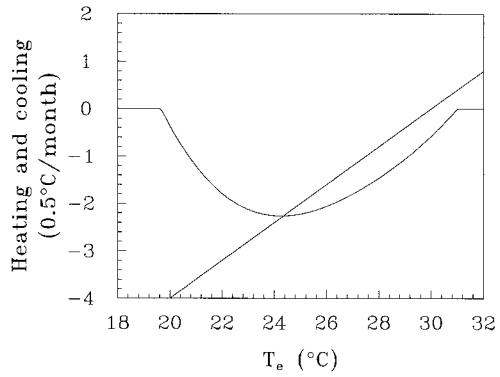

FIG. 1. Graphical steady-state solution to the coupled model for the Pacific Ocean basin. The warm pool is at radiative–convective equilibrium temperature $T_w = T_r = 30$°C. Net heating (reversed sign, straight line) and dynamical cooling (curve) in the eastern basin are plotted vs T_e under ocean dynamic equilibrium ($dh_w/dt = 0$). The equilibrium temperature of the eastern Pacific is indicated by the intersection point. The other model parameters were chosen as $\varepsilon_T = 1/(150$ days), $r = 1/(300$ days), $T_{r0} = 18$°C, $H_m = 50$ m, $H = 100$ m, $z_0 = 75$ m, $h^* = 50$ m, $\mu/H_m = 0.15/2$°C month^{-1}, $\mu bL/\alpha = 12.5$ m/°C, $\Delta T = 1$°C, $a_d = 0$, and $\mu_H = 0$.

Intensification of the easterly wind stress leads to the building up of the western Pacific warm pool, whereas a reduction of easterly wind stress results in the discharge of the warm pool. A similar equation can be approximately derived from shallow water dynamics with proper eastern and western boundary conditions for equatorial oceanic Kelvin and Rossby waves and approximations of filtering out wave propagating processes (Jin 1997b).

Equations (1)–(10) form a coupled conceptual model for the tropical Pacific. When the zonal advection in the SST [Eq. (1a)] and the Hadley circulation feedback to the equatorial zonal wind stress in Eq. (4) are ignored by setting $a_d = 0$ and $\mu_{\rm H} = 0$, the coupled model reduces to the simpler version of Jin (1996).

3. Pacific cold tongue and ENSO

The steady state of the conceptual coupled model is defined as the model climate state. For the simple version without zonal advection ($a_d = 0$) and Hadley circulation feedback ($\mu_{\rm H} = 0$), the steady-state solution of the eastern Pacific SST (T_e) can be determined by the balance between the thermodynamical heating and dynamic cooling of the eastern Pacific. By using Eqs. (9) and (10), the equilibrium thermocline depth of the eastern Pacific is found as $bL\tau/2$, which can be expressed as a function of T_e. Therefore, both thermodynamical heating [the first term of Eq. (1b)] and dynamic cooling [the second term of Eq. (1b)] of the eastern Pacific can be expressed as functions of the model eastern Pacific SST. The solution of equilibrium eastern Pacific SST is then graphically determined as shown in Fig. 1. In this particular equilibrium state, the cold tongue temperature is about 24.5°C, and the net heating rate is about 1.2°C

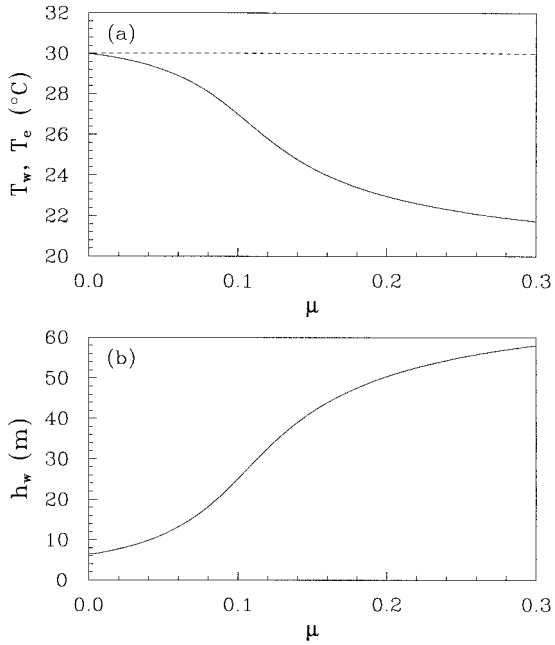

FIG. 2. The dependence of steady-state solution (dashed curve for T_w and solid curve for T_e in the upper panel, and h_w in low panel) on the dynamical coupling coefficient μ (in unit of 25 m/°C month^{-1}). The other parameters are the same as in Fig. 1.

per month, which is equivalent to a net surface heat flux of about 80 W m^{-2} for a mixed-layer depth of 50 m. The warm pool temperature remains at radiative equilibrium temperature of 30°C.

The coupled dynamics are found to be essential for the formation of the cold tongue (Dijkstra and Neelin 1995; Jin 1996). This is clearly illustrated in Fig. 2a, which presents the dependence of the nonlinear steady state on the dynamical coupling coefficient parameter μ. When this dynamical feedback coefficient is zero, the atmosphere and ocean become decoupled and tropical SST stays with zonal equilibrium. As the dynamical feedback increases, the eastern Pacific SST significantly decreases (Fig. 2a) while the east–west contrast in thermocline depth increases (Fig. 2b). When the coupling coefficient becomes excessively strong ($\mu > 0.2$), the model cold tongue temperature becomes unrealistically low.

The linear stability of the steady state can be analyzed by calculating the eigenvalues of the linearized version of the coupled model with respect to the steady state. In the case with $a_d = 0$ and $\mu_H = 0$, the instability and oscillation mechanisms of the ENSO associated with the Pacific cold tongue state can be highlighted by the linearized conceptual model as shown in Jin (1996):

$$\frac{dh'_w}{dt} = -rh'_w - rbL\mu T'_e/2,$$

$$\frac{dT'_e}{df} = RT'_e + \gamma h'_w, \qquad (11)$$

where

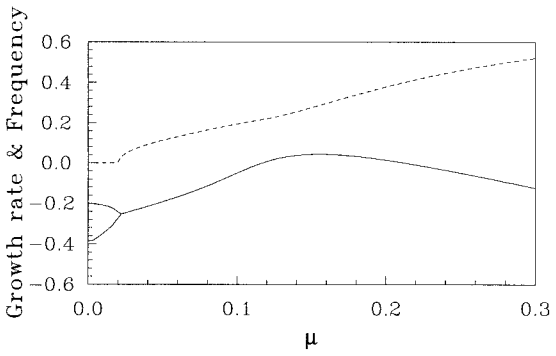

FIG. 3. The corresponding growth rates (solid lines) and frequency (dashed line) of the eigenmodes of the coupled model linearized with respect to the steady solutions in Fig. 2. The other parameters are the same as in Fig. 1. The unit for the growth rate and frequency is (2 mo)$^{-1}$.

$$R = -\varepsilon_T \frac{\varepsilon}{1+\varepsilon} + (\gamma bL\mu - M(\overline{w})/H_m),$$

$$\varepsilon = \Delta T/(T_r - \overline{T}_e), \qquad \gamma = \frac{M(\overline{w})}{H_m}\partial\overline{T}_{se}/\partial\overline{h}_e. \qquad (12)$$

The overbars and primes in Eqs. (11) and (12) denote the steady state and derivations from the steady state respectively, ε is the ratio between wind stress components due to the external easterly and Walker circulation of the steady state, γ denotes the sensitivity of the subsurface temperature to the thermocline depth, and R collectively represents Bjerknes feedback processes for the SST growth rate. When $R = r$, the growth rate of the ENSO mode is zero, whereas $R > r$ ($R < r$) the growth rate of the mode is positive (negative). The frequency at neutral growth rate ($R = r$) is $\sqrt{r\gamma bL\mu/2 - r^2}$, which depends heavily on $r\gamma bL\mu/2$, a term that combines the thermocline feedback (γ) and the recharge mechanism ($rbL\mu/2$). The Pacific cold tongue state is unstable when R is positive and overtakes the damping rate (r) in the ocean adjustment. The strong thermocline feedback is crucial for such an instability because Ekman pumping feedback alone is clearly unable to overcome the restoration damping. This linear system is basically the same as the linear conceptual recharged oscillator model, a systematically reduced form of the Cane–Zebiak type model (Jin 1997a,b) under a specific climate state. The out-of-phase relationship between an SST anomaly of the eastern Pacific and a thermocline depth anomaly of the western Pacific results from the recharge/discharge of the equatorial heat content associated with slow ocean dynamic adjustment, which is fundamental to the cyclic behavior of the ENSO as hypothesized by BWCZ and elucidated by Jin (1996, 1997a,b).

The linear stability of the Pacific cold tongue state solutions in Fig. 2 is illustrated in Fig. 3. Accompanying the cold tongue formation in the eastern Pacific as the dynamical coupling coefficient increases, the two un-

coupled modes, the decaying SST mode, and the ocean adjustment mode, merge to form an oscillatory ENSO mode. The ENSO mode is unstable in the parameter range from a moderate to relatively strong dynamical coupling. When the dynamical coupling parameter is small ($\mu < 0.11$), the system has a weak cold tongue state, which only gives rise to a damped ENSO mode because the thermocline feedback factor γ is small due to the weak upwelling in the basic state. When the dynamical coupling parameter is very large ($\mu > 0.22$), a resultant very strong cold tongue also gives rise to a damped ENSO mode because of a small γ due to the weak stratification (the reduction in $\partial\overline{T}_{se}/\partial\overline{h}_e$) under a very shallow eastern Pacific thermocline in the basic state. Therefore, neither a too weak nor a too strong cold tongue state can support an unstable ENSO mode.

The period in the unstable range is 3–5 years. A simple reference to this periodicity is provided by the period at neutral stability. Near neutral instability, $\gamma bL\mu \sim \overline{w}/H_m$, and the critical period can be estimated as $2\pi/\sqrt{(r\overline{w}/H_m)/2 - r^2}$. Clearly, the period of the ENSO depends basically on the two essential timescales of the climate system, the ocean dynamical adjustment timescale ($1/r$) and the upwelling timescale ($H_m/\overline{w}$) of the climate state. For instance, near the first Hopf bifurcation as shown in Fig. 3, the upwelling timescale is about 2 months, and the ocean adjustment timescale is set as 10 months; these lead to the critical period of about 5 years. It should be noted that both frequency and growth rate of the ENSO mode of the model depend on the ocean adjustment timescale. From Eqs. (11) and (12), for each steady solution, the growth (or decay) rate of the coupled mode depends linearly on the ocean adjustment rate, whereas the frequency is nearly proportional to its square root. The slower the ocean adjustment, the slightly more unstable the system is and the longer the period of the ENSO of the coupled system.

The dependence of ENSO mode on the dynamical coupling parameter shown in Fig. 3 differs from the results obtained from anomaly coupled models in which the basic state does not change with parameters. As shown by Jin (1997a), the leading mode of the CZ-type model, which shares the same linear dynamics as Eqs. (11), breaks down into two nonoscillatory modes and gives rise to a purely growing mode as the dynamical coupling becomes excessively strong. However, the leading mode in the fully coupled system does not split into nonoscillatory modes. Instead, it becomes a damped oscillatory mode as the dynamical coupling is very strong (Fig. 3). In the regime of moderate coupling where the model has a reasonable cold tongue climate state, these two types of coupled models are both capable of capturing the ENSO mode.

The oscillatory range and the periodicity of the ENSO mode indicated by the linear eigenanalysis agree well with what are obtained by nonlinear time integrations (Fig. 4). The self-sustained oscillatory regime is embraced by two supercritical Hopf bifurcations. The first

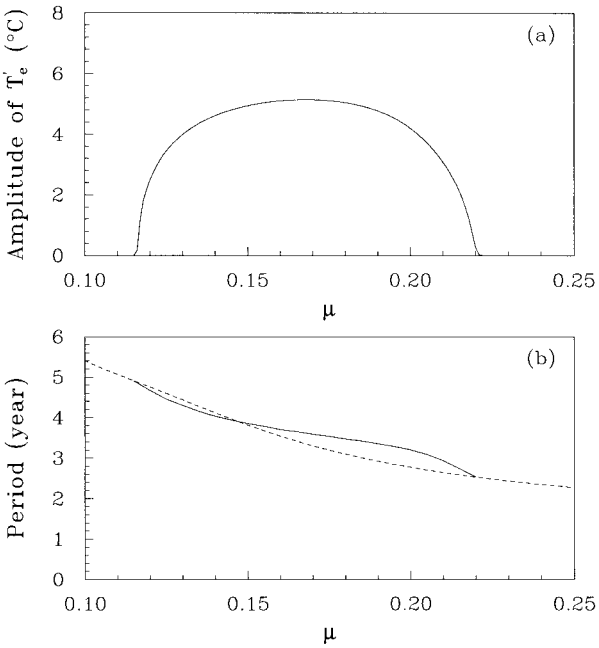

FIG. 4. The dependence of the amplitudes (a) and periods (b) of nonlinear oscillatory solutions on dynamical coupling coefficient μ. The dashed curve in the lower panel is linear periods inverted from the results in Fig. 3. The other parameters are the same as in Fig. 1.

one occurs as the dynamical coupling coefficient increases from weak to moderate. The amplitude of the nonlinear solution increases in proportion to the square root of supercriticality as the coupling coefficient exceeds its critical value, which is universal to the supercritical Hopf bifurcations (e.g., Ghil and Childress 1987; Jin 1997a). A similar supercritical Hopf bifurcation occurs when the dynamical coupling coefficient is changed from strong coupling toward relative moderate coupling in a backward manner. The critical period at the Hopf bifurcation at lower coupling is longer than that at stronger coupling because the latter features a colder climate state with a shorter upwelling rate. Near the first Hopf bifurcation, the dependence of amplitude and period on the dynamical coupling coefficient is similar to that analyzed by Jin (1997a) in a nonlinear coupled anomaly model with a prescribed basic state. However, the fully coupled model behaves very differently from the coupled anomaly model at a strong coupling regime. The supercritical backward Hopf bifurcation at strong coupling in Fig. 4 does not exist in the coupled anomaly model of Jin (1997a). Instead, through a pitchfork bifurcation, in addition to the prescribed climate state, there are two other equilibrium states: an anomalously warm SST and an extremely cold SST in the eastern Pacific. Clearly, this artificial multiplicity in equilibrium solutions is eliminated when full coupling is taken into consideration as first pointed out by Neelin and Dijkstra (1995).

Under the same parameter setting for the model

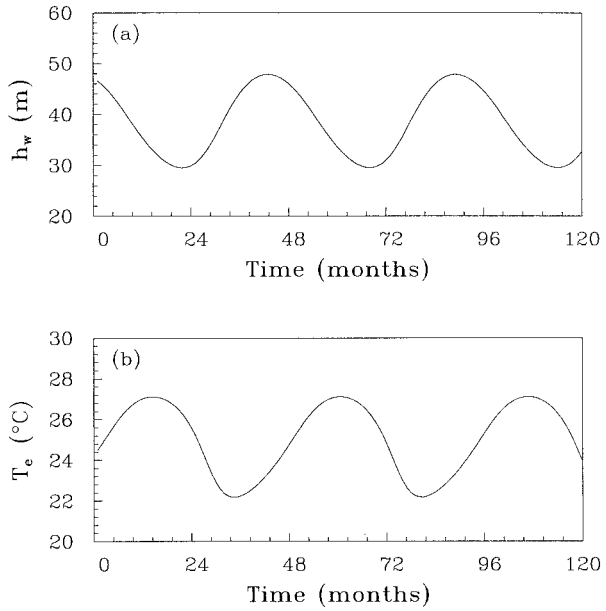

FIG. 5. Time series of h_w (in meters: a) and T_e (b) of the oscillatory solution under the same parameter setting as in Fig. 1.

steady state as shown in Fig. 1, the oscillatory solution (Fig. 5) clearly shows fluctuations about a 4-yr period in the cold tongue temperature and western thermocline depth. Outside the range of self-sustained oscillation, the system has a wide range for a slightly decaying oscillatory mode, which will produce substantial ENSO-like variability if it is stochastically excited (e.g., Jin 1997a).

The intensity of the cold tongue and its stability are also sensitive to the SST restoration rate (ε_T) and external wind stress. The restoration rate, collectively describing thermodynamical feedback processes involving sensible, latent, and radiative heating, is of great uncertainty. One particular example is the role of important feedback of stratus clouds in the heat balance over the cold tongue region. When SST is cold enough, stratus clouds will be formed locally. The stratus clouds further cool the SST due to the reduced solar radiation to the ocean surface. As shown by a number of recent studies (Philander et al. 1996; Li and Philander 1996; Ma et al. 1996), this positive feedback process has significant impact on the cold tongue intensity and its annual cycle. To represent such a process with the collective thermodynamics parameter ε_T will generally make ε_T as a function of SST because the feedback of stratus clouds to SST is nonlinear. Nevertheless, the effect of the stratus clouds can still be understood simply through the sensitivity of the cold tongue to the variation of ε_T. It can be shown that a steady-state solution of the model depends on (μ/ε_T); the quantitative impact of ε_T on the steady state can be inferred from Fig. 2. For instance, if ε_T is changed from 1/2.5 [corresponding to $(5\text{ mo})^{-1}$ in dimensional units] to 1/2 or to 1/3 and μ is fixed at 0.15, the corresponding steady-state solutions can be obtained from Fig. 2, which has a fixed ε_T at 1/2.5 by changing μ from 0.15 to 0.12 or to 0.2. Clearly, these changes lead to an increase or a decrease of the cold tongue temperature by nearly 1.5°C. The positive feedback effect of stratus cloud is equivalent to a reduction in ε_T. Thus, the stratus cloud feedback intensifies the cold tongue. Conversely, if there is a strong restoration to the radiative–convective equilibrium, then it will allow less dynamical feedback and thus lead to a weaker warm pool/cold tongue SST contrast.

The dependence of stability of the steady state on ε_T cannot be simply rescaled from Fig. 3. It is found that the frequency of the ENSO mode is insensitive to the changes in ε_T, whereas its growth rate depends on ε_T. The ENSO mode is unstable only in a certain moderate range for ε_T (not shown). A too large (small) thermodynamic damping results in a too weak (strong) cold tongue state, which does not support an unstable ENSO mode.

In the case discussed above, the explicit Hadley circulation feedback is turned off by setting $\mu_H = 0$. The external wind stress τ_{EX} thus can be interpreted more broadly as either a prescribed Hadley circulation or a component resulting from other sources such as the tropical land-locked convective heating over the maritime continents. When τ_{EX} [or ΔT in the Eq. (7)] is zero, the system has two equilibrium solutions, a symmetric thermodynamical equilibrium solution (not shown) and a cold tongue/warm pool solution. When τ_{EX} is an easterly wind stress, the symmetrical state is destroyed and the system only has a cold tongue steady-state solution as shown in Fig. 6. As this external wind stress increases, the cold tongue intensifies. The dependence of growth rate of the ENSO mode on τ_{EX} (Fig. 7) indicates an excessive τ_{EX} reduces the growth rate of ENSO-mode of a coupled system because it tends to create a too strong cold tongue. As discussed above, either a too weak or too strong cold tongue state is stable.

The impact of the Hadley circulation feedback on the steady state and its stability can be explored also by varying μ_H and setting $\tau_{EX} = 0$. When μ_H varies from 0.0 to 0.3 and $T_n = 20$°C, the results are almost the same as shown in Figs. 6 and 7 with ΔT changing between 0° and 2°C. In other words, τ_H has a similar impact on the solution of the coupled model as τ_{EX} is interpreted as a prescribed Hadley circulation component. This is because τ_H depends largely on the meridional difference in radiative–convective equilibrium temperatures, and the part of τ_H involving coupled feedback is relatively small in this model.

When the SST zonal advection is taken into consideration ($a_d \neq 0$), the western Pacific temperature cannot remain in radiative–convective equilibrium. Dynamical cooling due to the cold advection is balanced by thermodynamical warming, which tends to bring the SST of the western Pacific to radiative–convective equilibrium. This dynamic cooling effect, which reduces the

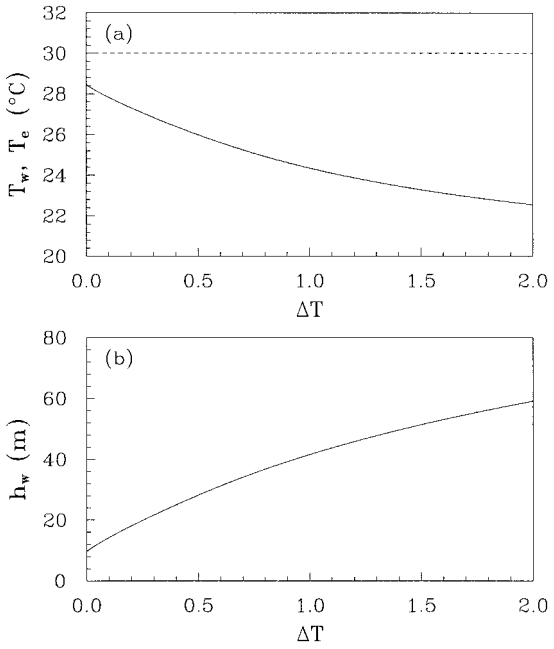

FIG. 6. As in Fig. 2 except that the sensitivity parameter is ΔT (in unit of °C) and μ/H_m is fixed at 0.15/2°C month^{-1}. The other parameters are the same as in Fig. 1.

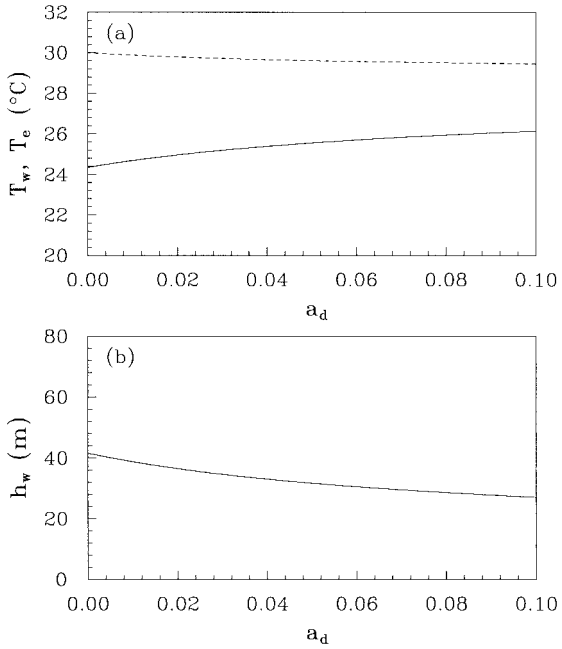

FIG. 8. As in Fig. 2 except that the sensitivity parameter is a_d and μ/H_m is fixed at 0.15/2°C month^{-1}. The other parameters are the same as in Fig. 1.

warm pool temperature, was recently suggested by Sun and Liu (1996) as a dynamic thermostat mechanism. The sensitivity of the Pacific cold tongue to the zonal advection can be illustrated by changing the parameter a_d, which measures the effectiveness of zonal advective feedback. By considering the Ekman flow as the equatorial surface current, a_d is a relatively small nondimensional number around 0.04 (see appendix). When zonal advection becomes effective as a_d increases, the warm pool SST decreases and the cold tongue SST increases (Fig. 8). The influence of the zonal advection in cold tongue SST is more effective than that in warm pool SST because the cold tongue SST is heavily controlled by dynamical feedback. The decrease in east–west SST contrast leads to a reduction in the Walker circulation and the related upwelling and shallower thermocline depth in the east Pacific. These chain reactions reduce the dynamical cooling in the eastern Pacific and therefore weaken the cold tongue. Therefore, the advective feedback acts as a negative feedback, which reduces instability of the ENSO mode. This is clearly shown in Fig. 9, which presents the dependence of the instability of the model climate state on the zonal advection parameter a_d. When a_d increases, the period of the ENSO mode slightly decreases (Fig. 9).

With the zonal advective feedback, the warm pool SST also exhibits an oscillatory solution, which propagates from the eastern Pacific through the westward advection (Fig. 10). In reality, the zonal advection is likely important only in the central Pacific. With our crude two-box approximation, the zonal advective cooling of the SST of the entire western Pacific is small. As long as the advective feedback is not excessive, its

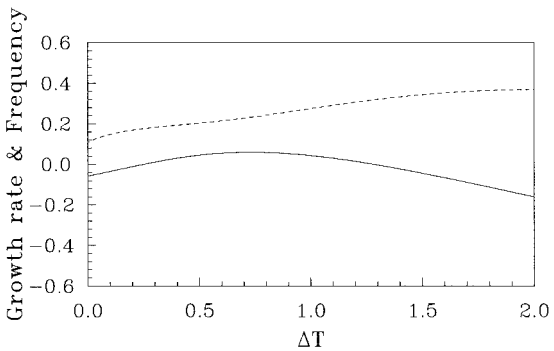

FIG. 7. As in Fig. 3 except for the solutions in Fig. 6.

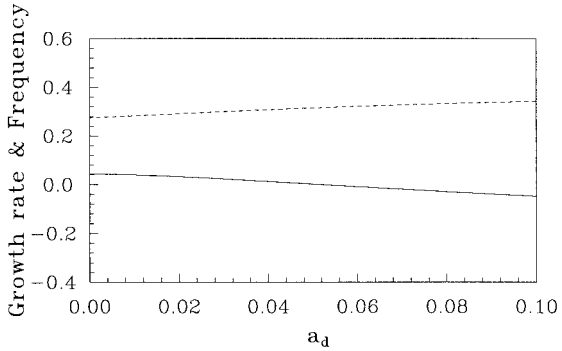

FIG. 9. As in Fig. 3 except for the solutions in Fig. 8.

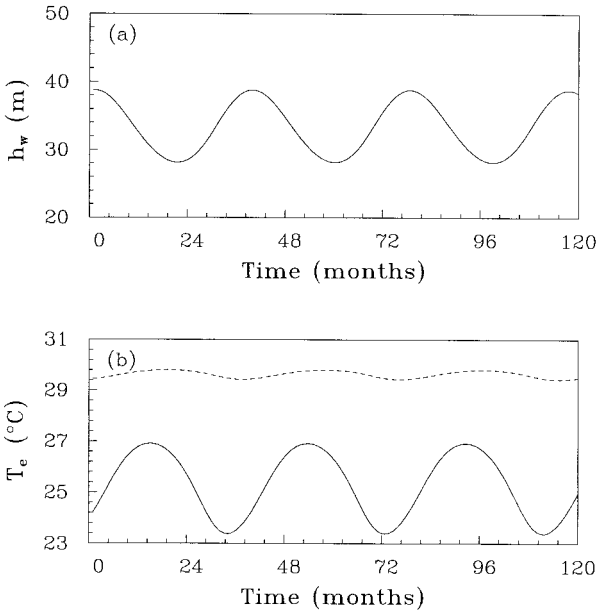

FIG. 10. Time series of h_w (in meters: a), T_e (solid curve in b), and T_w (dashed curve in b) of the oscillatory solution with $a_d = 0.04$, whereas the other parameters are the same as in Fig. 1.

impact on the warm pool/cold tongue climate state of the Pacific and ENSO variability is limited. In the western Pacific, the small dynamical cooling is in balance with a small thermodynamical heating, consistent with the observation of small climatological mean heat flux over the warm pool region.

4. Climate states of the equatorial Atlantic and Indian Oceans

The coupled system [Eqs. (1)–(10)] can be used to describe the basic features of climate states of the equatorial Atlantic and Indian Oceans by changing a few parameters. Three major differences between the Pacific and the Atlantic are considered here. First, the size of the equatorial Atlantic ocean is about one-third of that of the Pacific. Because the east–west thermocline contrast depends on the zonally integrated wind stress over the entire basin, the smaller size of the Atlantic Ocean results in a reduction of the east–west thermocline contrast for the same intensity of wind stress. Thus, the dynamical cooling in the eastern Atlantic becomes weaker than that in the eastern Pacific because of a deeper thermocline. Second, the Atlantic is more affected by the wind stress resulting from the heating sources over landmasses. The Walker circulation with its ascending motion over the Amazon region provides a significant contribution to the easterly wind over the equatorial Atlantic. Third, the zonal advection feedback in the Atlantic more effectively reduces both the warm pool SST and east–west SST contrast because its smaller size makes the zonal advective timescale shorter than that in the Pacific.

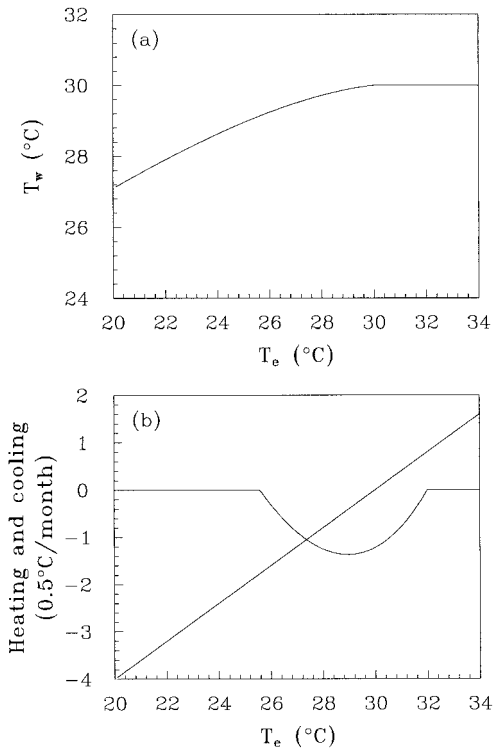

FIG. 11. Graphical steady-state solution to the coupled model for the Atlantic Ocean basin with zonal advective feedback. Top panel shows the relation T_e and T_w under the constraints of $dT_w/dt = 0$ and $dh_w/dt = 0$. The lower panel plots the net heating (reversed sign, straight line) and dynamical cooling in the eastern basin (curve) vs T_e using the relation in the upper panel and the constraint of $dh_w/dt = 0$. The intersection point in the lower panel gives the equilibrium solution of T_e, which also determines the solution of T_w using the upper panel. The model parameters are the same as for the Pacific case in Fig. 1 except that L (thus $\mu bL/\alpha$) is reduced into one-third of that for the Pacific case, $a_d = 0.12$ and $\Delta T = 3$°C.

The above three major factors can be incorporated into the model by setting the basin size to be one-third of that for Pacific sector, enlarging the external easterly wind by a factor of 3 to account for the contribution resulting from the heating over the Amazon region, and increasing the advective feedback parameter a_d inversely to the reduction of the basin size. With these changes in the model parameters, the climate state solution for the equatorial Atlantic Ocean is illustrated in Fig. 11. The Atlantic warm pool/cold tongue contrast is about 2.5°C and the warm pool temperature is cooler than the radiative equilibrium temperature by nearly 0.7°C. The heat fluxes required for the steady state are about 40 and 10 W m^{-2} in the eastern and western Atlantic, respectively. This climate state of the Atlantic Ocean is similar to that in Jin (1996), and the minor difference results from the increase in the external easterly wind component, the decrease in the basin size, and inclusion of zonal advection in the present model.

In the case for the Atlantic, one factor that has not been taken into consideration is the impact of the zonal-

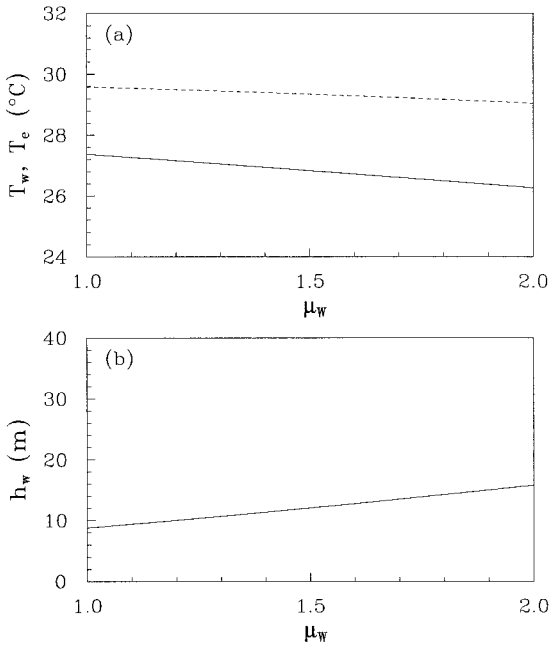

FIG. 12. The dependence of steady-state solution (dashed curve for T_w and solid curve for T_e in the upper panel, h_w in low panel) on the nondimensional relative coupling parameter μ_W for the Atlantic case. The other parameters are the same as in Fig. 11.

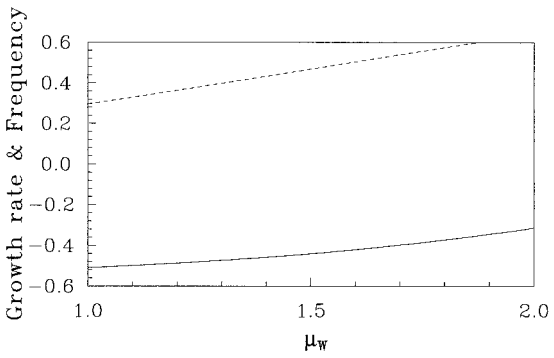

FIG. 13. The corresponding growth rates (solid line) and frequency (dashed line) of the eigenmodes of the coupled model linearized with respect to the steady solutions in Fig. 12. The other parameters are the same as in Fig. 11. The unit of the growth rate and frequency is $(2\ \text{mo})^{-1}$.

scale dependence of the response of the coupled Walker circulation to the zonal SST contrast. This scale dependence is nonlinear. When the zonal scale is small, the subsidence warming and heat loss of atmosphere over the cold tongue region are largely in balance, thus the coupled Walker circulation is proportional to SST contrast and its zonal scale. When the zonal scale is large, friction and thermodynamic damping in the atmosphere become important in both momentum and heat balances, and the coupled Walker circulation is proportional to SST contrast but inversely proportional to its zonal scale. To test the sensitivity of this scale dependence, we rewrite Eq. (7) as

$$\tau = -\frac{\mu}{\alpha}\{\mu_w(T_w - T_e) + \Delta T\} \qquad (13)$$

by introducing a nondimensional factor μ_W, which is unity for the Pacific and the baseline Atlantic case shown in Fig. 11. The dependence of the Atlantic cold tongue and warm pool temperature on μ_W, as shown in Fig. 12, indicates that a large μ_W, representing a strong coupled Walker circulation response to SST contrast, will reduce both the cold tongue and warm pool temperature, whereas the east–west contrast seems not to be sensitive to μ_W. It is plausible that due to the small size of the Atlantic, μ_W is somewhat larger than 1. However μ_W is smaller than 3 because of the nonlinear scale dependence as argued above. Clearly, a larger μ_W will result in stronger reduction of the western Atlantic temperature because of stronger zonal advective cooling in the model. Thus the so-called dynamical thermostat effect is likely stronger in the Atlantic than in the Pacific.

The Atlantic climate state in Fig. 12 is stable and the leading oscillatory eigenmode is heavily damped as shown in Fig. 13. Such a damped mode cannot give rise to a pronounced ENSO-like oscillation except with strong external excitations. This is consistent with the finding that there is much less pronounced interannual variability over the tropical Atlantic (Zebiak 1993).

The situation of the Indian Ocean is different from the Atlantic in the external zonal wind component. A weak westerly wind component, resulting from the Walker circulation associated with the western Pacific warm pool and the Maritime Continent, is dominant over the Indian Ocean. This westerly wind stress can prohibit dynamical cooling because of Ekman downwelling at the equator as suggested by Jin (1996). For instance, by setting $\Delta T = -1$°C to represent a weak external westerly wind component and otherwise keeping other parameters the same as for the equatorial Atlantic case in Fig. 11, the system has only one steady-state solution, which presents the stable radiative–convective equilibrium state without an east–west SST contrast (Fig. 14). This zonal symmetric climate state for the Indian Ocean is consistent with the observation that the annual-mean equatorial Indian SST is nearly zonally uniform except for a colder equatorial SST near the Somali coast due to coastal upwelling. The dynamical coupled processes, which create the zonal asymmetry of warm pool/cold tongue contrast in the Pacific and Atlantic, are largely disabled in the equatorial Indian Ocean because of the external westerly wind resulting from the Walker circulation ascending at the western Pacific warm pool and maritime continent.

5. Discussions and conclusions

In this paper, a conceptual model is constructed to describe the basic coupled dynamics of the tropical ocean–atmosphere interaction. It incorporates the pos-

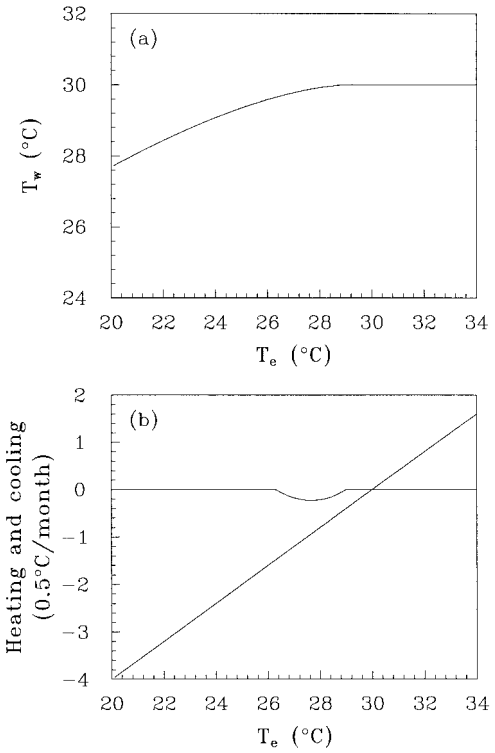

FIG. 14. Graphical steady-state solution to the coupled model for the Indian Ocean basin. Parameters are the same as for the Atlantic case except $\Delta T = -1$°C.

itive feedback processes, which are responsible for the formation of the Pacific cold tongue and the growth of a warm or cold phase of the ENSO, and memory residing in the ocean dynamic adjustment that is essential for the phase transition of the ENSO.

The dynamical coupling among the zonal SST and thermocline depth contrasts and equatorial easterly surface wind is essential for the generation of the Pacific cold tongue. The strong eastern Pacific cold tongue is maintained by the balance between the thermodynamical heating due to the surface heat flux and dynamical cooling resulting from upwelling of cold subsurface water into the surface layer. The subsidence of the strong coupled Walker circulation over the cold tongue results in adiabatic heating to balance the heat loss from the atmosphere to the cold tongue. Because of the lack of oceanic dynamical cooling, the Pacific warm pool may be viewed as decoupled from the asymmetrical coupled dynamics to the first order with its temperature at radiative–convective equilibrium. This is consistent with the fact that there is little observed net heat flux through the warm pool ocean surface (Esbensen and Kushnir 1981) and the atmosphere over the warm pool is nearly moist neutral (Emanuel et al. 1994) with the adiabatic cooling from the ascending motion of Walker circulation largely balanced by latent heating.

The intensity of the Pacific cold tongue depends strongly on the dynamical coupling coefficient and the thermodynamical restoration rate. Under a moderated coupling coefficient, the Pacific cold tongue state has a reasonable intensity. However, it becomes too weak (strong) when the coupling coefficient is too small (large). The dependence of the cold tongue intensity on the restoration rate, which collectively represents all the thermodynamical feedback processes in the radiative, latent, and sensible heating fluxes, is inversely equivalent to the dependence of the cold tongue intensity on the dynamical coupling. Modest changes in either the coupling coefficient or the thermodynamical restoration rate can lead to significant changes in the intensity of the Pacific cold tongue and its stability. For instance, the positive feedback of stratus clouds to SST can significantly reduce the collective thermodynamical damping of SST in the cold tongue region and therefore intensify cold tongue amplitude. The sensitivity of cold tongue state to the coupling coefficient and the thermodynamical restoration rate are most likely responsible for the scatter of the coupled models in simulating both the climate state and ENSO of the tropical climate system.

The Pacific cold tongue is unstable and supports an ENSO-like oscillation over a wide range centered around a modest dynamical coupling coefficient. Outside this range, the cold tongue becomes either too strong or too weak to support the instability of the ENSO mode. The unstable regime of the Pacific cold state is the ENSO regime, which is embraced by two supercritical Hopf bifurcations. The first one occurs at a relatively weak coupling and the second in a backward manner at a strong coupling. The ENSO mode of the coupled system can be delineated by a simple linearized system with respect to different model steady-state solutions for various parameters. The slow physics of the ENSO mode can be explained by the recharge oscillator mechanism (Jin 1996, 1997a). The period of oscillation can be understood from linear analysis. In particular, the periods at the Hopf bifurcations are $2\pi/\sqrt{(r\overline{w}/H_m)/2 - r^2}$, depending on the ocean adjustment timescale and the upwelling timescale of the climate state. Dynamical coupling combines the two timescales into ENSO periodicity within the range of 3–5 years.

The equatorial easterly wind resulting from either external forcing or the Hadley circulation breaks the zonal symmetry of the coupled system because it creates east–west contrasts in SST and thermocline depth. Although the strong zonal asymmetry in SST and thermocline depth is largely attributed to the coupled dynamics, the inclusion of this easterly wind stress component unrelated to zonal SST contrast eliminates the possibility for the system to have an additional zonal symmetric state. Quantitatively, this easterly wind component also enhances the Pacific cold tongue and alters the stability of the ENSO model of the coupled system through its modification to the cold tongue state.

Zonal advection of SST reduces the western Pacific warm pool SST, as suggested by Sun and Liu (1996).

It also increases the cold tongue SST. The reduction in east–west SST contrast weakens the Walker circulation and thus the dynamical cooling feedback. Therefore, the cold advection acts as a negative feedback in the tropical atmosphere–ocean interaction. However, the cold advective feedback is relatively weak because the horizontal advection rate is much smaller than the vertical advection rate. Qualitatively, the effect of the cold zonal advection on the Pacific climate state and the ENSO is limited.

Applying the conceptual model to the equatorial Atlantic and Indian Ocean sectors, the results suggest that for the Atlantic Ocean, there is only a weak cold tongue climate state that is stable and cannot support an ENSO-like oscillation. The smaller basin size of the equatorial Atlantic Ocean, the stronger zonal advective feedback, and the impact of a stronger external easterly wind resulting from the heating source over the adjacent landmasses are likely responsible for the Atlantic climate state and its stability being significantly different from those of the Pacific system. For the Indian Ocean, the weak westerly wind associated with the Walker circulation over the warm pool of the western Pacific basically prohibits the asymmetric coupled dynamics, and thus the climate state maintains a zonally uniform warm state without an equatorial cold tongue.

The simple model highlights the basic physical mechanisms responsible for the formation of the Pacific climate state and ENSO and the totality of coupled dynamics of interannual variabilty and the climate states of the equatorial ocean basins. It also captures the major differences among the three tropical ocean sectors and produces the basic climate states for each of these subsystems. However, the tropical climate system is not a linear combination of the individual subsystems. In addition to the important basin–basin interaction and ocean–atmosphere–land interaction implied in this study, the annual monsoon circulation, or more generally the whole annual cycle of the tropical climate system, can play a significant role in shaping the tropical climate and its variability. Our understanding of the totality of coupled dynamics of the global Tropics will be enriched as a more comprehensive paradigm comprising all these fundamental aspects of the tropical climate emerges.

Acknowledgments. This work was supported by National Science Foundation Grant ATM-9312888 and ATM-9615952 and by National Oceanographic and Atmospheric Administration Grant GC95773. The author thanks Roger Lukas, Bin Wang, and Thomas Schroeder for their valuable comments, which led to the improvement of the manuscript, and Diane Henderson for her careful editing of the manuscript.

APPENDIX

Ekman Flow Advection

Following the formulation of Zebiak and Cane (1987), the dynamical balance of the Ekman flow, which is assumed to dominate the surface flow in the equatorial ocean, can be expressed as

$$-fv = \tau_x - \varepsilon_s u$$
$$fu = \tau_y - \varepsilon_s v, \tag{A1}$$

where u, v are the zonal and meridional velocity of the surface flow; τ_x and τ_y are zonal and meridional wind stress forces per unit mass; and ε_s is the momentum damping rate. The Ekman pumping velocity w in the mixed layer with the depth of H_m is

$$w = H_m\left(\frac{\partial u}{\partial x} + \frac{\partial v}{\partial y}\right). \tag{A2}$$

Near the equator, the zonal flow can be approximately expressed as $u \sim \tau_x/\varepsilon_s$, and the meridional divergence can be expressed as $\partial v/\partial y \sim -\beta\tau_x/\varepsilon_s^2$ under the assumption that τ_y is small. Thus, the equatorial zonal advection rate and upwelling rate in the Eqs. (1a) and (1b) of the text can be approximately expressed as

$$-u/(L/2) = -\tau_x\beta/\varepsilon_s^2 a_d, \qquad w/H_m \sim -\tau_x\beta/\varepsilon_s^2(1 + a_d),$$
$$a_d = \varepsilon_s/(\beta L/2). \tag{A3}$$

Given ε_s about 1/(2 days), $L/2 \sim 7.5 \times 10^6$ m, and $\beta = 2.3 \times 10^{-11}$/(m s), the nondimensional parameter a_d is about 0.03–0.04. This crude estimation indicates that the vertical advective timescale is much shorter than the zonal advective timescale due to the dominant contribution of the meridional divergence to the equatorial upwelling.

REFERENCES

Anderson, D. L. T., and J. P. McCreary, 1985: Slowly propagating disturbances in a coupled ocean–atmosphere model. *J. Atmos. Sci.,* **42,** 615–629.

Barnett, T. P., N. Graham, M. Cane, S. Zebiak, S. Dolan, J. O'Brien, and D. Legler, 1988: On the prediction of El Niño of 1986–1987. *Science,* **241,** 192–196.

——, M. Latif, E. Kirk, and E. Roeckner, 1991: On ENSO physics. *J. Climate,* **4,** 487–515.

Battisti, D. S., 1988: The dynamics and thermodynamics of a warming event in a coupled tropical atmosphere/ocean model. *J. Atmos. Sci.,* **45,** 2889–2919.

——, and A. C. Hirst, 1989: Interannual variability in the tropical atmosphere/ocean system: Influence of the basic state and ocean geometry. *J. Atmos. Sci.,* **46,** 1687–1712.

Bjerknes, J., 1969: Atmospheric teleconnections from the equatorial Pacific. *Mon. Wea. Rev.,* **97,** 163–172.

Cane, M. A., and S. E. Zebiak, 1985: A theory for El Niño and the Southern Oscillation. *Science,* **228,** 1084–1087.

——, ——, and S. C. Dolan, 1986: Experimental forecasts of El Niño. *Nature,* **321,** 827–832.

Dijkstra, H. A., and J. D. Neelin, 1995: Ocean–atmosphere interaction and the tropical climatology. Part II: Why the Pacific cold tongue is in the east. *J. Climate,* **8,** 1343.

Emanuel, K. A., J. D. Neelin, and C. S. Bretherton, 1994: On large-scale circulations in convecting atmospheres. *Quart. J. Roy. Meteor. Soc.,* **120,** 1111–1143.

Esbensen, S. K., and Y. Kushnir, 1981: The heat budget of the global ocean: An atlas based on estimates from surface marine observations. Climate Res. Inst. Rep. 29, Dept. of Atmos. Sci., 220

pp. [Available online at http://ats.ors.edu/Faculty/esbensen/tropical/CRI_Report_29.html]
Ghil, M., and S. Childress, 1987: *Topics in Geophysical Fluid Dynamics: Atmospheric Dynamics, Dynamo Theory, and Climate Dynamics.* Springer-Verlag, 485 pp.
Jin, F.-F., 1996: Tropical ocean–atmosphere interaction, the Pacific cold tongue, and the El Niño–Southern Oscillation. *Science,* **274,** 76–78.
——, 1997a: An equatorial ocean recharge paradigm for ENSO. Part I: Conceptual model. *J. Atmos. Sci.,* **54,** 811–829.
——, 1997b: An equatorial ocean recharge paradigm for ENSO. Part II: A stripped-down coupled model. *J. Atmos. Sci.,* **54,** 830–847.
——, and J. D. Neelin, 1993: Modes of interannual tropical ocean–atmosphere interaction—A unified view. Part I: Numerical results. *J. Atmos. Sci.,* **50,** 3477–3502.
——, ——, and M. Ghil, 1996: El Niño/Southern Oscillation and the annual cycle: Subharmonic frequency locking and aperiodicity. *Physica D,* **98,** 442–465.
Latif, M., T. P. Barnett, M. A. Cane, M. Flügel, N. E. Grahem, H. von Storch, J.-S. Xu, and S. E. Zebiak, 1994: A review of ENSO prediction studies. *Climate Dyn.,* **9,** 167–179.
Li, T., and S. G. H. Philander, 1996: On the annual cycle of the eastern equatorial Pacific. *J. Climate,* **9,** 2986–2998.
Ma, C.-C., C. R. Mechoso, A. W. Robertson, and A. Arakawa, 1996: Peruvian stratus clouds and the tropical Pacific circulation: A coupled ocean–atmosphere GCM study. *J. Climate,* **9,** 1635–1645.
Mechoso, C. R., and Coauthors, 1995: The seasonal cycle over the tropical Pacific in coupled ocean–atmosphere general circulation models. *Mon. Wea. Rev.,* **123,** 2825–2838.
Neelin, J. D., 1991: The slow sea surface temperature mode and the fast-wave limit: Analytic theory for tropical interannual oscillations and experiments in a hybrid coupled model. *J. Atmos. Sci.,* **48,** 584–606.
——, and H. A. Dijkstra, 1995: Ocean–atmospheric interaction and the tropical climatology. Part I: The danger of flux-correction. *J. Climate,* **8,** 1325–1342.
——, M. Latif, and F.-F. Jin 1994: Dynamics of coupled ocean–atmosphere models: The tropical problem. *Annu. Rev. Fluid Mech.,* **26,** 617–59.
——, D. S. Battisti, A. C. Hirst, F.-F. Jin, Y. Wakata, T. Yamagata, and S. Zebiak, 1998: ENSO theory. *J. Geophys. Res.*, in press.
Philander, S. G. H., 1990: *El Niño, La Niña, and the Southern Oscillation.* Academic Press, 293 pp.
——, T. Yamagata, and R. C. Pacanowski, 1984: Unstable air–sea interactions in the tropics. *J. Atmos. Sci.,* **41,** 604–613.
——, R. C. Pacanowski, N. C. Lau, and M. J. Nath, 1992: A simulation of the Southern Oscillation with a global atmospheric GCM coupled to a high-resolution, tropical Pacific Ocean GCM. *J. Climate,* **5,** 308–329.
——, D. Gu, D. Halpern, G. Lambert, N.-C. Lau, T. Li, and R. C. Pacanowski, 1996: Why the ITCZ is mostly north of the equator. *J. Climate,* **9,** 2958–2972.
Rasmusson, E. M., and J. M. Wallace, 1983: Meteorological aspects of the El Niño/Southern Oscillation. *Science,* **222,** 1195–1202.
Schopf, P. S., and M. J. Suarez, 1988: Vacillations in a coupled ocean–atmosphere model. *J. Atmos. Sci.,* **45,** 549–566.
Suarez, M. J., and P. S. Schopf, 1988: A delayed action oscillator for ENSO. *J. Atmos. Sci.,* **45,** 3283–3287.
Sun, D., and Z. Liu, 1996: Dynamic ocean–atmosphere coupling: A thermostat for the tropics. *Science,* **272,** 1148–1149.
Wyrtki, K., 1985: Water displacements in the Pacific and the genesis of El Niño cycles. *J. Geophys. Res.,* **91,** 7129–7132.
Zebiak, S. E., 1993: Air–sea interaction in the equatorial Atlantic region. *J. Climate,* **6,** 1567–1586.
——, and M. A. Cane, 1987: A model El Niño–Southern Oscillation. *Mon. Wea. Rev.,* **115,** 2262–2278.